Observation of Termination Process of Long Pulse Plasma Discharges Using Stereoscopic Fast Framing Cameras in the Large Helical Device*)

Mamoru SHOJI, Hiroshi KASAHARA, Hirohiko TANAKA, Takanori MURASE, Masahiko TOKITANI, Shigeru MORITA, Motoshi GOTO, Tetsutaro OISHI, Takashi MUTOH, Eduardo DE LA CAL[1)], Calros HIDALGO[1)] and the LHD Experiment Group

National Institute for Fusion Science, 322-6 Oroshi-cho, Toki 509-5292, Japan
[1)]*Centro de Investigaciones Energéticas, Medioambientales y Tecnológicas, 40 Avenida Complutense, Madrid 28040, Spain*

(Received 23 November 2015 / Accepted 11 March 2016)

Long pulse discharges in the Large Helical Device (LHD) were interrupted by the emission of large amounts of carbon dusts released from a closed helical divertor in the previous experimental campaign (FY2013). In order to control the dust emission, the configuration of the closed divertor near lower and upper ports was modified in the last experimental campaign (FY2014). While the modification of the divertor configuration has successfully controlled the release of dusts, long pulse discharges were often terminated with abrupt increase in iron ion emission. The termination process of a long pulse plasma discharge was observed with a stereoscopic fast framing camera which can identify the three-dimensional positions of dusts. It proved that the dusts penetrated into the main plasma through the plasma periphery, which could induce the radiation collapse in the plasma discharge.

Keywords: long pulse discharge, stereoscopic observation, dust, fast framing camera, LHD

DOI: 10.1585/pfr.11.2402056

1. Introduction

Steady state plasma discharge operation (SSO) is essential for future nuclear fusion reactors. The Large Helical Device (LHD) in the National Institute for Fusion Science (NIFS) is the largest super-conducting helical machine in the world [1]. The LHD has advantage over tokamaks for steady-state plasma discharge operation because of no plasma instabilities induced by the toroidal plasma current such as disruptions and ELMs, etc. The magnetic configuration for plasma confinement is formed by external super conducting coils which inherently produce an ergodic layer and divertor legs around the main plasma confinement region inside of the Last Closed Flux Surface (LCFS). Long pulse plasma discharges in LHD are a good test-stand for investigating physical phenomena in SSO in nuclear fusion reactors under a saturated vacuum wall condition without particle pumping effect.

However, SSO has been performed in some superconducting tokamaks [2, 3], the termination process of the plasma discharges has not yet fully been investigated because of the necessity of huge data storage memories with high time resolution. In LHD, several fast framing cameras have been applied to the investigation of the termination process of the plasma discharges using an end trigger mode operation for the camera observation.

In the previous experimental campaign in FY2013, a long pulse discharge up to ∼48 minutes under a condition of a heating power of ∼1.2 MW and a line-average electron density of $\sim 1.2 \times 10^{19}\,\mathrm{m}^{-3}$ was successfully achieved. It was found that the plasma discharge was suddenly interrupted with the abrupt increase in carbon ion emission (CIII). The termination process of the plasma discharge was observed with a monocular fast framing camera installed in an upper port (4.5-U). It showed that the large amounts of dusts were released from a closed divertor region in the inboard side of the torus near a lower port (4.5-L) just before the plasma termination [4].

In the LHD vacuum vessel, divertor plates are installed along the two lines of the strike points [5]. In the closed divertor configuration, the most of the divertor plates in the inboard side are mounted so as to face inward in order to make neutral particles released from the divertor plates are transported to the inlets of a cryo-sorption pump installed behind a dome structure [6]. At the edges of the closed divertor near lower and upper ports, target plates are installed to intersect one of the divertor legs in order to concentrate the positions of the strike points to the inboard side for efficient neutral particle pumping [7].

Divertor regions near the lower and upper ports are tightly enclosed by the dome structure and the target plates. After the previous experimental campaign, the traces of

author's e-mail: shoji@LHD.nifs.ac.jp
*) This article is based on the presentation at the 25th International Toki Conference (ITC25).

the exfoliation of carbon-rich mixed material deposition layers were found on the enclosed areas [8]. Just before the plasma termination, the observation with the monocular fast framing camera suggests that the dusts exfoliated from the enclosed area penetrated into the main plasma confinement region through the ergodic layer. In the last experimental campaign in FY2014, the termination process of a long pulse discharge induced by dust emission was observed with a stereoscopic fast framing camera. It makes the identification of the three-dimensional positions of the dusts possible at the plasma termination [9].

In this paper, the stereoscopic observations just before the termination of the plasma discharge are presented. The analysis of the three-dimensional positions of the dusts observed with the stereoscopic fast framing camera is also shown, which is followed by summary.

2. Experimental Setup for Stereoscopic Observation

The long pulse plasma discharges have been sustained with Ion Cyclotron Range of frequency Heating (ICH) and with Electron Cyclotron resonance Heating (ECH) [10]. A stereoscopic fast framing camera has been installed in an outer port (3-O). Optical lenses were mounted at two separated positions in the outer port as shown in Fig. 1 (a). The images viewed from the two lens positions are transferred and combined with a bifurcated silica-based coherent image fiber mounted at the front of the fast framing camera (Photron FASTCAM SA-X). The images from the two lenses mounted at the left and right sides on the outer port are projected to the left and right half side on a CMOS image sensor in the camera, respectively. The viewing area of the stereoscopic camera includes isotropic graphite (carbon) divertor plates and helical coil cans covered with stainless steel armor tiles in the inboard side of the torus as illustrated in Fig. 1 (b). The divertor configuration in this area remained an open configuration in the last experimental campaign. Some fiducial points were set on the surface of the armor tiles on the helical coil can locating in the viewing area for accurate measurement of the positions of dusts. The three-dimensional positions of the fiducial points had been measured on the site before the last experimental campaign.

3. Time Evolution of Plasma Parameters just before the Termination of a Long Pulse Discharge

Before the last experimental campaign, the closed helical divertor configuration near the lower and upper ports was modified in order to control the deposition layers in the enclosed area [11]. In the original divertor configuration, most of sputtered impurities (carbon) from the target plates directed toward the enclosed area. In the new divertor configuration, the shape of some target plates has been rearranged such that most of the impurities are released to the main plasma by changing the direction of the front surface of the target plates

After this modification, the termination of long pulse discharges due to the release of the large amounts of dusts from the enclosed area was not observed in the last experimental campaign. The traces of the exfoliation of the deposition layers were also not found in the enclosed area. Instead, some long pulse discharges were interrupted with abrupt increase in iron ion emission, which are possibly not related to the modification of the divertor configuration. Figure 2 shows the time evolution of the electron density, radiation power and impurity ion emission just before the termination of a long pulse discharge. It shows that the increase in the iron ion emission (FeXVI) is more rapid than that in carbon ion emission (CIII) at the time of the initial phase of the electron density rise. The abrupt increase in the radiation power is synchronized with that in the iron ion emission, suggesting that the plasma was interrupted by the sudden influx of iron from outside of the plasma, which is different from that in the previous long pulse discharge in which abrupt increase in carbon ion emission was observed just before the termination [4].

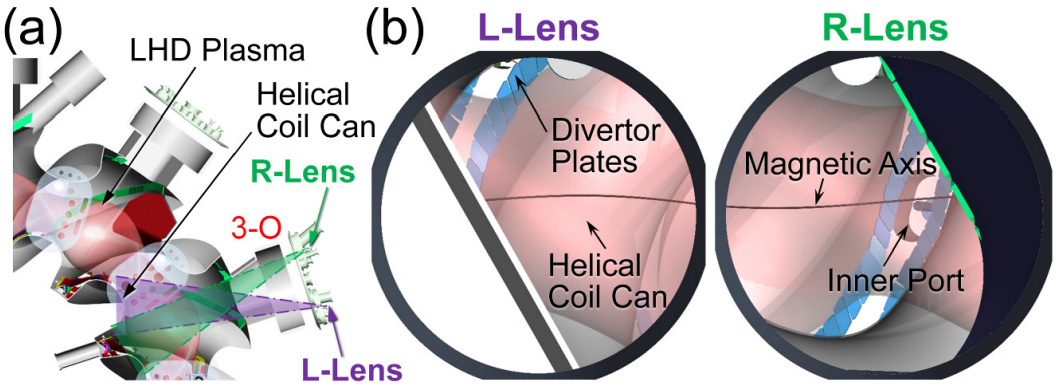

Fig. 1 Top view of the configuration of a stereoscopic fast framing camera installed in an outer port (3-O) (a), and the field of views of the stereoscopic camera from the positions of the two (left and right) optical lenses (b).

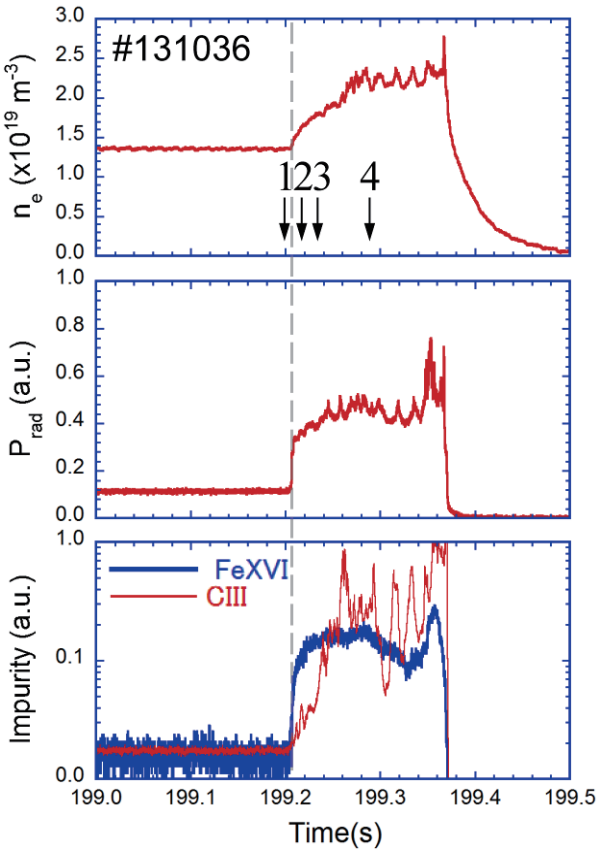

Fig. 2 Time evolution of the electron density, radiation power and impurity ion emission just before the termination of a long pulse discharge in the last experimental campaign. Small black arrows indicate the times of the images in Fig. 3.

4. Stereoscopic Observation of the Termination Process of a long Pulse Discharge

The termination process of the long pulse discharge was observed with the stereoscopic fast framing camera at a rate of 1,000 fps. Figure 3 gives the sequential images of the plasma just before the termination of the plasma discharge. The first image (the upper-left one) shows that a bright spot appeared on a point on the surface of an armor tile on a side wall of a helical coil can in the inboard side of the torus. After the bright spot expanded as shown in the second image with sparks, some dusts, which are identified as incandescent small bright spots, were released from the surface of the helical coil can near the equatorial plane. In the last image (the lower-right one), it seems that some large sized dusts (shown as big bright spots) penetrated into the main plasma.

These stereoscopic images can provide the three dimensional positions of the dusts using a pin-hole camera model [12] and the information of the three-dimensional positions of the fiducial points. Figures 4 (a) and (b) present the perspective and top views of the three-dimensional positions of observed dusts (colored squares) and the ergodic layer (small white dots). It shows that the most of the observed dusts locate in the inboard side of the torus near the ergodic layer. The figure also indicates that the most of the dusts locate around a position where the LHD plasma is horizontally elongated shown by a black broken line in Fig. 4 (b), which enables the dust positions to be approximately projected to the poloidal cross-section at the plasma horizontally elongated position.

Figure 5 shows the positions of the observed dusts projected to the poloidal cross-section of the LHD plasma

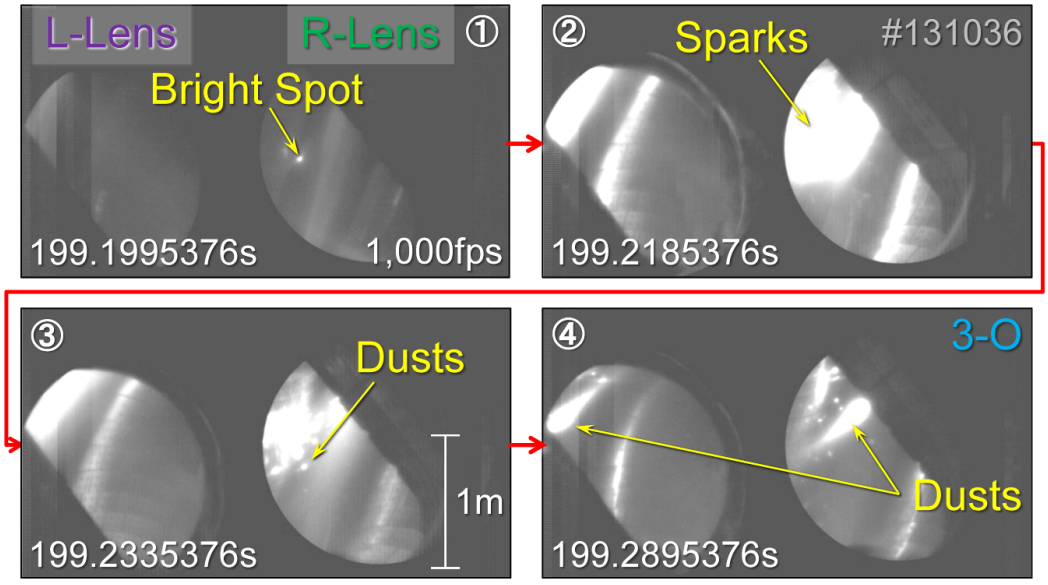

Fig. 3 Four sequential images of a plasma observed with a stereoscopic fast framing camera just before the termination of a long pulse discharge in the last experimental campaign.

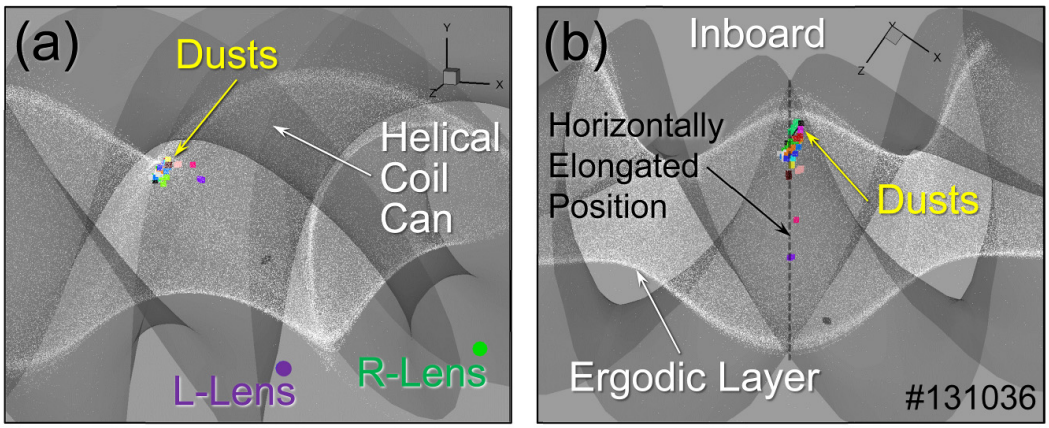

Fig. 4 Perspective (a) and top (b) views of the three-dimensional positions of dusts observed with a stereoscopic fast framing camera just before the termination of a long pulse discharge in the last experimental campaign. The positions of the dusts and the ergodic layer are indicated as colored squares and small white dots, respectively.

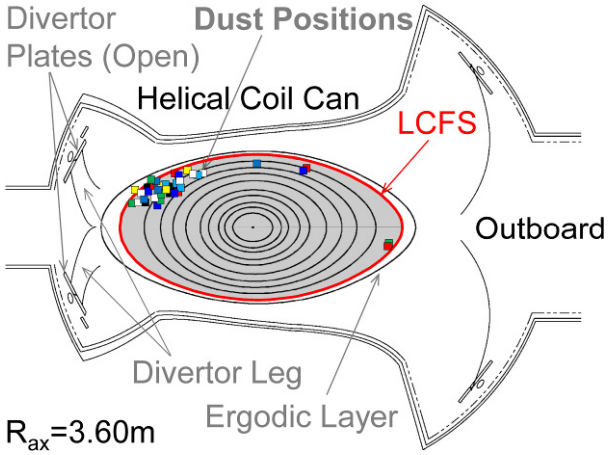

Fig. 5 Poloidal cross-section of the magnetic configuration of an LHD plasma for R_{ax} = 3.60 m and the observed dust positions projected to the cross-section where the LHD plasma is horizontally elongated.

for the most typical magnetic configuration in long pulse discharges in which the radial position of the magnetic axis R_{ax} is 3.60 m. It indicates that the dusts locate inside of the LCFS and penetrates into the main plasma confinement region. The dusts reach to the position where the normalized minor radius ρ is about 0.8. The observation with the stereoscopic fast framing camera firstly proved that the dusts, which were released from the armor tiles, penetrated into the main plasma just before the termination of the plasma discharge. Considering the experimental results of impurity transport studies using a Tracer Encapsulated Solid PELlet (TESPEL) injector [13], it is probable that ionized iron atoms evaporated from the surface of the iron dusts in the main plasma are transported to the core plasma, which induced radiation collapse and led to the termination of the long pulse discharge.

5. Summary

Modification of the configuration of the target plates in the closed helical divertor has successfully controlled the termination of long pulse discharges due to the emission of the large amounts of carbon dusts from the enclosed area. However, long pulse discharges were interrupted with abrupt increase in iron ion emission. The emission of dusts released from the surface of an armor tile on a helical coil can was observed with a stereoscopic fast framing camera just before the plasma termination. It proved that the observed dusts penetrate into the main plasma confinement region through the ergodic layer to induce the radiation collapse of the plasma discharge.

Acknowledgments

This work is financially supported by a NIFS budget (NIFSULPP015) and is performed with the support and under the auspices of the NIFS Collaboration Research program (NIFS12KNXN236). It is performed by NIFS/NINS under the project of Formation of International Scientific Base and Network (KEIN1111), and this work is also supported by the A3 foresight program for study on critical physics issues specific to steady state sustainment of high-performance plasmas.

[1] A. Komori *et al.*, Fusion Sci. Technol. **58**, 1 (2010).
[2] D. Vanhoutte *et al.*, Nucl. Fusion **44**, L11 (2004).
[3] M. Sakamoto *et al.*, Nucl. Fusion **44**, 693 (2004).
[4] M. Shoji *et al.*, Nucl. Fusion **55**, 053014 (2015).
[5] S. Masuzaki *et al.*, Fusion Sci. Technol. **50**, 361 (2006).
[6] M. Shoji *et al.*, Plasma Fusion Res. **7**, 2405145 (2012).
[7] M. Shoji *et al.*, J. Nucl. Mater. **415**, 557 (2011).
[8] M. Tokitani *et al.*, J. Nucl. Mater. **463**, 91 (2015).
[9] M. Shoji *et al.*, J. Nucl. Mater. **463**, 861 (2015).
[10] T. Mutoh *et al.*, Nucl. Fusion **53**, 063017 (2013).
[11] M. Shoji *et al.*, Contrib. Plasma Phys. (accepted).
[12] R. Sakamoto *et al.*, Rev. Sci. Instrum. **76**, 103502 (2005).
[13] S. Sudo *et al.*, Plasma Fusion Res. **8**, 2402059 (2013).